

Intrinsic Flux-Flow Resistance Steps in the Cuprate Superconductor $\text{Nd}_{2-x}\text{Ce}_x\text{CuO}_y$

O. M. Stoll,¹ S. Kaiser,¹ R. P. Huebener,¹ and M. Naito²

¹Physikalisches Institut, Lehrstuhl Experimentalphysik II, Universität Tübingen, Morgenstelle 14, D-72076 Tübingen, Germany

²NTT Basic Research Laboratories, 3-1 Morinosato-Wakamiya, Atsugi-shi, Kanagawa, 243-01, Japan

(Received 23 June 1998)

We have observed a novel intrinsic step structure in the flux-flow resistance of epitaxial *c*-axis-oriented films of $\text{Nd}_{2-x}\text{Ce}_x\text{CuO}_y$ as a function of current at intermediate magnetic fields $B_{c1} \ll B < B_{c2}$. The effect is observed only if the sample is cooled with superfluid helium. For explaining the underlying instability, we propose a model based on the strongly energy-dependent density of states available near the Fermi energy for quasiparticle scattering in the superconducting mixed state for the clean limit. [S0031-9007(98)07278-0]

PACS numbers: 74.25.Fy, 74.60.Ge, 74.72.Jt

In the cuprate superconductors the electronic structure of the vortices in the mixed state is distinctly different from that in the classical superconductors, since the cuprates are characterized by an extremely small coherence length ξ and, therefore, reside in the clean or even superclean limit. The energy smearing $\delta\varepsilon = \hbar/\tau$ due to the mean electronic scattering time τ must be compared with the energy gap Δ in the single particle excitation spectrum and with the level spacing Δ^2/ε_F of the Andreev bound states in the vortex core. Here \hbar is Planck's constant divided by 2π and ε_F the Fermi energy. In the "moderately clean" limit we have $\Delta^2/\varepsilon_F \ll \delta\varepsilon \ll \Delta$, and in the "superclean" limit $\delta\varepsilon \ll \Delta^2/\varepsilon_F$, whereas $\Delta \ll \delta\varepsilon$ represents the "dirty" limit. In the classical superconductors we deal almost exclusively with the dirty limit. In this case a vortex can be described simply by a normal cylinder of radius ξ . In the cuprates such a simple picture does not apply any more.

In this paper we report on flux-flow resistivity measurements in epitaxial *c*-axis-oriented films of $\text{Nd}_{2-x}\text{Ce}_x\text{CuO}_y$ (NCCO) in the magnetic field regime $B_{c1} \ll B < B_{c2}$. NCCO appears favorable for such experiments because of its relatively small pinning effects compared to other cuprates. There is strong experimental evidence that this material represents a single-gap *s*-wave BCS type superconductor [1–3]. Recently, in NCCO films we have observed the logarithmic singularity in the flux-flow resistivity [4,5] predicted by Larkin and Ovchinnikov [6] in the low-temperature and low magnetic field limit. This singularity results from the shrinking of the vortex core with decreasing temperature ("Kramer-Pesch effect"). In contrast to our earlier measurements [4,5], our present experiments deal with the intermediate magnetic field regime where the interaction between vortices becomes important. Here, with increasing electric current we observe a novel intrinsic step structure of the flux-flow resistance combined with hysteretic behavior. We explain our results in terms of a strongly energy-dependent density of states (DOS) available for scattering. In the spirit of the tight binding approximation this energy-dependent DOS evolves at higher

magnetic fields from the energy spectrum of the isolated vortices [7–10].

Our experiments were performed with epitaxial *c*-axis-oriented films of NCCO grown by molecular beam epitaxy (MBE) on SrTiO_3 substrates [11,12]. The film thickness d was 90–100 nm. Two types of sample geometries have been fabricated using standard photolithography: (a) microbridges in four-point geometry with the dimensions $w = 20 \mu\text{m}$, $L = 200 \mu\text{m}$, and $w = 40 \mu\text{m}$, $L = 300 \mu\text{m}$ ($w = \text{width}$, $L = \text{length}$); (b) microbridges with four voltage leads of $30 \mu\text{m}$ width placed along the bridge with a spacing of $100 \mu\text{m}$ (total length between outer voltage leads $L = 360 \mu\text{m}$, $w = 40 \mu\text{m}$). This second type allows one to study the three sections of the same bridge separately. Its geometry is shown schematically in the inset of Fig. 1. We denote the voltage of the three sections of the bridge V_1 , V_2 , and V_3 , respectively (V_2 represents the middle section), and the total voltage of all three sections V_T (between the two outer leads). For measuring the electric sample resistance Ag contact pads have been deposited on the NCCO films,

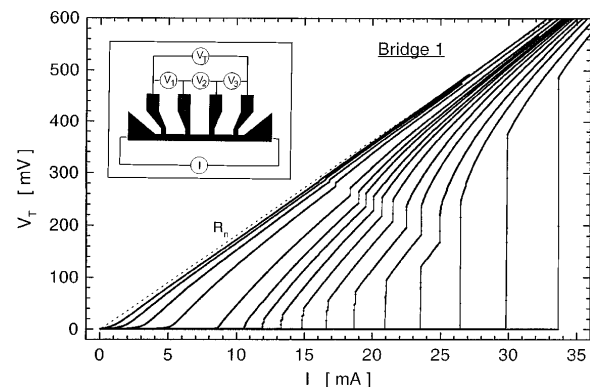


FIG. 1. Voltage V_T plotted versus current at different magnetic fields. From right to left B is increased in 100 mT steps covering the range $B = 800\text{--}1800$ mT and in 500 mT steps for $2000\text{--}4000$ mT ($T = 1.92$ K). The dotted line indicates the normal-state resistance. The inset shows the sample geometry of type (b).

and two 0.1 mm diameter Al wires were bonded to each pad. During all experiments the samples were immersed in liquid helium in order to minimize effects from Joule heating. The temperature was lowered below 4.2 K by pumping. Its value was obtained from the vapor pressure of the He bath. A superconducting magnet served for generating a magnetic field perpendicular to the film plane, i.e., parallel to the c axis of the NCCO.

In our measurements we have swept the current at a slow rate of about 0.5 mA/s, using a battery-powered current source controlled with an external ramp generator. The voltage signal was amplified by an SRS model SR 560 preamplifier and recorded with a personal computer, using an analog-to-digital converter driven with a sampling rate of 50 Hz. After each change of the magnetic field we have swept the current up to the normal conducting region to minimize effects from magnetic hysteresis. We have investigated a total of 9 NCCO samples (optimally doped with $x \approx 0.15$ or slightly overdoped with $x \approx 0.16$) all showing similar results. In the following we present typical results obtained for samples of type (b). These samples had the same critical temperature $T_c = 21.3$ K. They were slightly overdoped ($x \approx 0.16$). The resistive transition is shown in inset (a) of Fig. 2 for one sample. The resistivity values at 295 and 30 K were $\rho(295 \text{ K}) = 128 \mu\Omega \text{ cm}$ and $\rho(30 \text{ K}) = 18 \mu\Omega \text{ cm}$, respectively.

The most interesting novel feature of our results is the observation of a characteristic step structure of the voltage current characteristic (VIC) in the superconducting mixed state. In Fig. 1 we show a series of VIC's measured at $T = 1.92$ K at different magnetic fields in the range $B = 800$ –4000 mT. From right to left B is increased in 100 mT steps ($B = 800$ –1800 mT), and then for 2000–4000 mT in 500 mT steps. For $B \leq 1000$ mT we see a distinct voltage step, which splits into two steps at higher magnetic fields. The magnitude of these steps

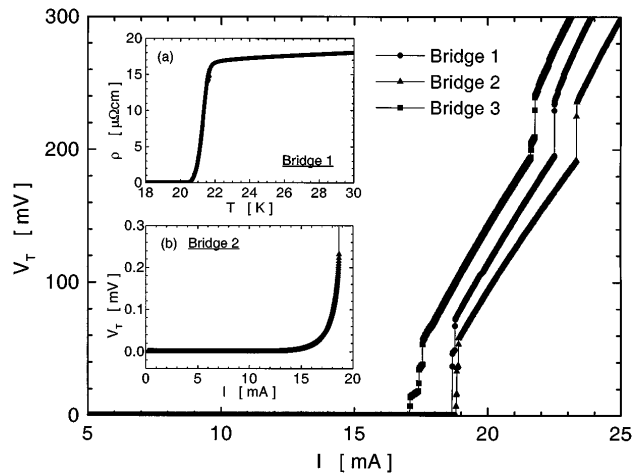


FIG. 2. Voltage V_T plotted versus current at higher voltage resolution at $B = 1300$ mT and $T = 1.92$ K for the same sample as shown in Fig. 1 and for two additional samples fabricated from the same epitaxial film. Inset (a) shows the resistive transition curve of one sample. Inset (b) shows the VIC of one sample at still higher resolution.

decreases in a characteristic way with increasing magnetic field. On their upper end all curves approach the normal state resistive behavior. In Fig. 2 we present data for the lower voltages at higher voltage resolution for the same bridge as shown in Fig. 1 and for two additional bridges ($T = 1.92$ K; $B = 1300$ mT). The three bridges were fabricated from the same epitaxial film encompassing angles of 60° and 120° , respectively, with each other (see inset of Fig. 4 below). Aside from some details, the main features of the step structure are very similar. The first step always appeared at a finite voltage [see inset (b) of Fig. 2 and the inset of Fig. 3].

The VIC's measured for the three sections of bridge 3 (see inset of Fig. 1) are shown separately in Fig. 3 ($T = 1.92$ K, $B = 1100$ mT). In addition to the voltages

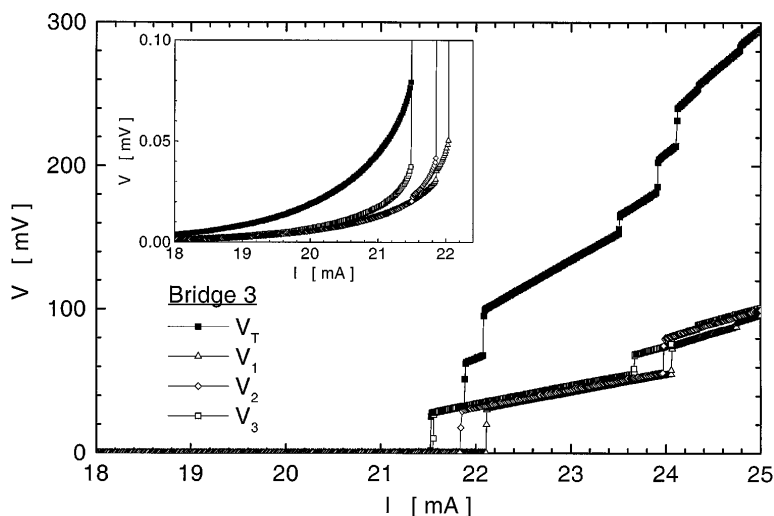


FIG. 3. Voltages V_1 , V_2 , V_3 of the three sections of one sample, and the total voltage V_T plotted versus current ($B = 1100$ mT, $T = 1.92$ K). The inset shows the VIC's at higher voltage resolution.

V_1 , V_2 , V_3 , we also display the total measured voltage V_T . Again, the inset shows the VIC's at higher resolution. The voltage V_T is seen to represent the superposition of the voltages from the three sections. The two major voltage steps as the main features in the three sections are very similar, the VIC's being only slightly shifted with respect to each other along the current axis. It is interesting that the geometric separation of our bridges into three individual sections appears to promote the formation of a single dissipative domain in each section.

The step structure in the resistive voltage suggests the presence of an instability, and one expects hysteresis. Indeed, in our current-biased measurements we always found hysteretic behavior, if the current is raised above the value where a voltage step appears, and subsequently is lowered again. Typical examples are shown in Fig. 4.

It is important to note that the detailed step structure seen in Figs. 1–4 can be observed only if the sample is immersed in superfluid helium, i.e., below the Λ point. Apparently, heating effects can easily wash out the detailed structure of the VIC's. Above the Λ point the VIC's do not show distinct steps any more. However, in superfluid He the detailed features are robust and exactly reproducible if the direction of the current and/or magnetic field is reversed, or if the measurements are repeated from one day to the next. Measurements of the derivative $\partial V/\partial I$ using a modulation amplitude of 10 μ A and a modulation frequency 1–50 kHz precisely confirm the detailed shape of the VIC's.

The experimental facts that we have described so far strongly suggest that we are dealing with a novel type of electronic instability affecting the flux-flow resistance. Turning to the explanation of our results it appears difficult to relate the observed step structure in the flux flow resistance to extrinsic effects and sample inhomogeneity, such as pinning, hot spot generation, etc. A model based

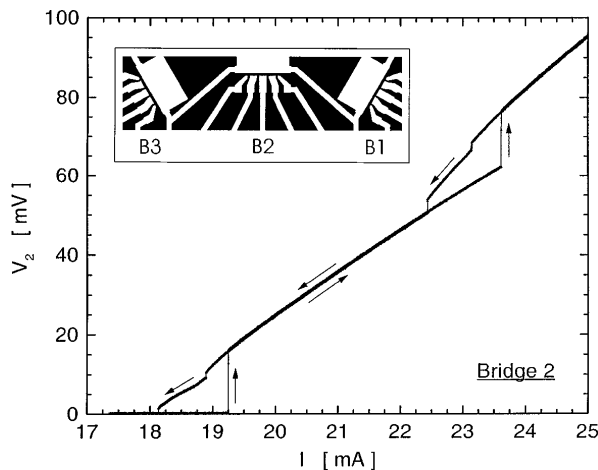


FIG. 4. Voltage V_2 versus current showing the typical hysteresis. The arrows indicate the current sweep direction. $B = 1300$ mT, $T = 1.92$ K. The inset shows the film with three bridges referred to in Fig. 2.

on hot spots would have difficulties with the fact that the resistance steps are observed only if the sample is immersed in superfluid helium. Instead, it appears that we are dealing with an intrinsic effect. These arguments are supported by the fact that the step structure in different samples or in the three sections of the same sample is nearly identical. We propose that the observed instability results from the nonlinear increase of the DOS with increasing distance $|\varepsilon - \varepsilon_F|$ available for quasiparticle scattering above and below the Fermi energy. Here we refer to the spatially averaged DOS in the superconducting mixed state. This has been discussed quasiclassically in the pure limit many years ago [13,14]. The energy dependence of the DOS $N(\varepsilon)$ has been found to increase symmetrically with respect to the Fermi energy ε_F . As essential ingredients of our model we assume that in the presence of the electric field F (generated by vortex motion) the quasiparticle distribution is strongly shifted away from equilibrium; i.e., the clean or superclean limit is valid. Further we assume that the energy dependence of the DOS of the static vortex lattice survives in a moving vortex lattice and the presence of an electric field. The latter assumption appears reasonable if the vortex lattice moves, coherently, as can be expected for large vortex velocities.

In the presence of the electric field F and in the low-temperature limit $T \ll \Delta/k_B$ the energy of the quasiparticles is shifted away from ε_F by the amount $eFv_F\tau$

$$\varepsilon = \varepsilon_F \pm eFv_F\tau \quad (1)$$

(v_F = Fermi velocity, τ = quasiparticle scattering time). Here + (–) refers to the electrons (holes). With increasing electric field more and more states above (below) the Fermi energy become populated (depopulated). This may also be described by a field-dependent effective temperature T^* of the quasiparticles. Because of the energy shift of the quasiparticles expressed in Eq. (1) and the increase of the DOS with increasing distance $|\varepsilon - \varepsilon_F|$ discussed above, the phase space $N(\varepsilon)$ for quasiparticle scattering increases with F , and the resistivity ρ becomes field dependent: $\rho(F) \sim N(\varepsilon)$. Here, for simplicity, we have considered only the contribution of the quasiparticles moving in the field direction. This is illustrated schematically in Fig. 5, where we have taken the functional dependence $N(\varepsilon)$ such that two steps in the VIC are generated, similar to our experimental observations. The two steps result from the shoulder in the DOS. If this shoulder were absent, only a single step would appear. We emphasize that our explanation of the step structure requires a nonlinear increase of $N(\varepsilon)$ with $|\varepsilon - \varepsilon_F|$, which emerges from the theoretical treatments performed up to now [13,14]. The function $N(\varepsilon)$ is expected to depend sensitively on the intervortex distance and, hence, on the flux density B . Therefore, the flux-flow resistance steps should also display a sensitive B dependence, in agreement with our observations.

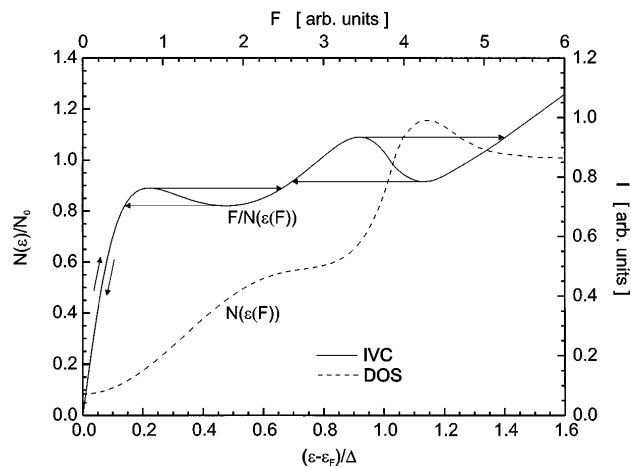


FIG. 5. Dashed line: Normalized DOS $N(\varepsilon)/N_0$ plotted versus $(\varepsilon - \varepsilon_F)/\Delta$. This curve is numerically taken such that it yields the VIC with two hysteretic voltage steps shown by the solid line and using the proportionality $I \sim F/N(\varepsilon(F))$.

From our model and the previous theoretical work [13,14], the strongly nonlinear behavior (instability) of F is expected for $|\varepsilon - \varepsilon_F| = eFv_F\tau \approx \Delta$. Taking $\Delta = 4$ meV [15] and $v_F = 10^7$ cm/s [16] for NCCO and using the value $V_T \approx 200$ mV for the appearance of the upper voltage step (see Figs. 1 and 2), we obtain $\tau = 6 \times 10^{-11}$ s. This value appears reasonable in view of the energy relaxation time $\tau_\varepsilon = 59 \times 10^{-11}$ s found earlier near 1.7 K from a study of the Kramer Pesch effect in the low-field limit [4,5]. Regarding the lower voltage step appearing at $V_T \approx 200$ μ V such an estimate presents some problem. However, it may be possible that the Kramer Pesch effect survives at the intermediate magnetic fields [17] or that the first step is associated with the minigap, yielding the condition $eFv_F\tau \approx \Delta^2/2\varepsilon_F$. Then a shoulder in $N(\varepsilon)$ such as shown in Fig. 5 may arise from such an origin. Our simplified model can provide a principle understanding of the underlying physics. However, other mechanisms, i.e., symmetry changes of the vortex lattice, may be involved. Clarification of this matter clearly requires further experimental and theoretical work.

In summary, a novel intrinsic step structure in the flux-flow resistivity of NCCO films has been observed as a

function of current if the sample is immersed in superfluid helium. For explaining the underlying electronic instabilities we propose a model based on the strongly energy-dependent DOS available for quasiparticle scattering in the superconducting mixed state for the clean limit.

Financial support by the Deutsche Forschungsgemeinschaft and many clarifying discussions with N. Schopohl are gratefully acknowledged. R. P. H. also acknowledges interesting discussions with M. Ichioka. T. Doderer and S. Kittelberger provided help during the initial part of the experiments.

- [1] D.H. Wu, J. Mao, S.N. Mao, J.L. Peng, X.X. Xi, T. Venkatesan, R. L. Greene, and S.M. Anlage, Phys. Rev. Lett. **70**, 85 (1993).
- [2] S.M. Anlage, D. Wu, J. Mao, X.X. Xi, T. Venkatesan, J.L. Peng, and R.L. Greene, Phys. Rev. B **50**, 523 (1994).
- [3] C.W. Schneider, Z.H. Barber, J.E. Evetts, S.N. Mao, X.X. Xi, and T. Venkatesan, Physica (Amsterdam) **233C**, 77 (1994).
- [4] S.G. Doettinger, S. Anders, R.P. Huebener, H. Haensel, and Yu.N. Ovchinnikov, Europhys. Lett. **30**, 549 (1995).
- [5] S.G. Doettinger, R.P. Huebener, and S. Kittelberger, Phys. Rev. B **55**, 6044 (1997).
- [6] A. I. Larkin and Yu.N. Ovchinnikov, Zh. Eksp. Teor. Fiz. **73**, 299 (1977) [Sov. Phys. JETP **46**, 155 (1977)].
- [7] C. Caroli, P.G. de Gennes, and J. Matricon, Phys. Lett. **9**, 307 (1964).
- [8] L. Kramer and W. Pesch, Z. Phys. **269**, 59 (1974).
- [9] W. Pesch and L. Kramer, J. Low Temp. Phys. **15**, 367 (1973).
- [10] F. Gygi and M. Schlüter, Phys. Rev. B **43**, 7609 (1991).
- [11] M. Naito, H. Sato, and H. Yamamoto, Physica (Amsterdam) **293C**, 36 (1997).
- [12] M. Naito and H. Sato, Appl. Phys. Lett. **67**, 2557 (1995).
- [13] U. Brandt, W. Pesch, and L. Tewordt, Z. Phys. **201**, 209 (1967).
- [14] A.L. Fetter and P.C. Hohenberg, in *Superconductivity*, edited by R.D. Parks (Marcel Dekker, New York, 1969), Vol. 2, p. 817.
- [15] S.M. Anlage *et al.*, Phys. Rev. B **50**, 523 (1994).
- [16] D.M. King *et al.*, Phys. Rev. Lett. **70**, 3159 (1993).
- [17] M. Ichioka (private communication).